PTS is activated by *ATF4* and promotes lung adenocarcinoma development via the Wnt pathway

Wei Ma[1#], Chao Wang[2#], Ruzhen Li[1], Zhaohui Han[1], Yuanzhu Jiang[1], Xiangwei Zhang[1], Duilio Divisi[3], Enrico Capobianco[4], Lin Zhang[1], Wei Dong[1,5]

[1]Department of Thoracic Surgery, Shandong Provincial Hospital Affiliated to Shandong First Medical University, Jinan, China; [2]Department of Respiratory, The First Affiliated Hospital of Shandong First Medical University, Jinan, China; [3]Department of Life, Health and Environmental Sciences, University of L'Aquila, Thoracic Surgery Unit, "Giuseppe Mazzini" Hospital of Teramo, Teramo, Italy; [4]The Jackson Laboratory, Farmington, CT, USA; [5]Department of Thoracic Surgery, Shandong Provincial Hospital, Cheeloo College of Medicine, Shandong University, Jinan, China

Contributions: (I) Conception and design: W Ma, C Wang; (II) Administrative support: R Li, W Dong; (III) Provision of study materials or patients: Z Han; (IV) Collection and assembly of data: X Zhang; (V) Data analysis and interpretation: L Zhang; (VI) Manuscript writing: All authors; (VII) Final approval of manuscript: All authors.

[#]These authors contributed equally to this work and should be considered as co-first authors.

Correspondence to: Wei Dong. Department of Thoracic Surgery, Shandong Provincial Hospital Affiliated to Shandong First Medical University, 324 Jingwu Road, Jinan 250021, China. Email: dr.dongwei@sdu.edu.cn.

Background: The effects and mechanism of 6-pyruvoyl-tetrahydropterin synthase (*PTS*) on lung adenocarcinoma (LUAD) were studied in LUAD cells and mice with subcutaneously transplanted tumors.

Methods: *PTS* level in tissues and cells was tested by immunohistochemistry, western blot, and quantitative real-time polymerase chain reaction (qRT-PCR). The impacts of *PTS* on cell viability, proliferation, apoptosis, invasion, and migration were determined by Cell Counting Kit-8 (CCK-8), colony formation assay, flow cytometry, transwell assay, and wound healing assay, respectively. The Cancer Genome Atlas (TCGA) analysis and dual luciferase assay were conducted to predict and verify the relationship between *PTS* and activating transcription factor 4 (*ATF4*). A mouse model was established by subcutaneous injection with cancer cells. Tumor volume was calculated as $V = ab^2/2$. Ki67 and terminal deoxynucleotidyl transferase dUTP nick end labeling (TUNEL) staining were used to measure cell proliferation and apoptosis in tumors.

Results: *PTS* was highly expressed in LUAD. Higher *PTS* level was correlated with late clinical stages and poor survival of patients. Down-regulation of PTS inhibited the viability and proliferation and induced apoptosis of LUAD cells. *PTS* was activated by *ATF4*, and up-regulation of *ATF4* reversed the inhibitory effect of *PTS* silencing on LUAD cells. Silencing of *PTS* inhibited the Wnt pathway. Down-regulation of *PTS* inhibited tumor growth in mice.

Conclusions: *PTS* was highly expressed in LUAD. PTS was activated by *ATF4* and promoted LUAD development via the Wnt pathway.

Keywords: 6-pyruvoyl-tetrahydropterin synthase (*PTS*); lung adenocarcinoma (LUAD); activating transcription factor 4 (*ATF4*); Wnt pathway

Introduction

Lung cancer includes mainly two subtypes: non-small cell lung cancer (NSCLC), which accounts for 85% of lung cancers, and small cell lung cancer. Lung adenocarcinoma (LUAD) is the main subtype of NSCLC, accounting for about 60% of all NSCLC cases (1-3). Many potential therapeutic targets and corresponding targeted drugs have been discovered and applied in clinics for the treatment of LUAD, including epidermal growth factor receptor (EGFR), fibroblast growth factor receptor, and insulin-like growth factor (4-6). Nevertheless, there is an urgent need to discover more potential and effective target genes in LUAD to further improve the treatment strategy.

The 6-pyruvoyl-tetrahydropterin synthase (*PTS*) gene was cloned by Thöny *et al.* in 1992 and is located at 11q22.3-23.3 (7). At present, research on *PTS* is mainly focused on its effect on tetrahydrobiopterin deficiency (BH₄D), which is caused by a lack of *PTS* (8). *PTS* gene levels are relevant to newborn screening, as a lack of *PTS* can lead (8): (I) a BH4 synthesis disorder, resulting in accumulation of phenylalanine; (II) a lack of L-dopa, epinephrine, 5-hydroxytryptophan, and other physiologically active substances; (III) a decreased nerve cell myelin protein synthesis and immunity. The *PTS* gene has been rarely studied in cancer. Zhao *et al.* (9) reported that *PTS* is up-regulated in early colorectal cancer; however, there has been no prior research on *PTS* expression in LUAD.

In order to study the upstream mechanism of PTS in lung cancer, we predicted the transcription factors upstream of PTS by bioinformatics analysis, and finally screened 7 transcription factors. Activating transcription factor 4 (*ATF4*) was selected according to the high prediction score and their correlation with PTS expression in The Cancer Genome Atlas (TCGA)-LUAD. *ATF4*, which belongs to the cAMP-response element binding (CREB) protein family, is activated by many stimuli, including oxygen deficiency, amino acid deficiency, endoplasmic reticulum stress, oxidative stress, and growth factor regulatory proteins (10,11). The role of *ATF4* in lung cancer has been investigated, but its effect remains controversial. Du *et al.* (12) found that *ATF4* may promote lung cancer cell proliferation and invasion, while Zhang *et al.* (13) reported that *ATF4* promotes Noxa-dependent apoptosis in LUAD cells treated with andrographolide. The Wnt gene was first discovered as a proto-oncogene (int) in mice in 1982 and renamed Wnt due to its homology with the *Drosophila* wingless gene reported by Sharma (14). The Wnt pathway participates in embryonic development and some normal physiological processes, as well as in the induction and regulation of a variety of tumors, including lung cancer (15,16). Here, we focused on the function of *PTS* in LUAD, hypothesizing that *PTS* is activated by *ATF4* and promotes LUAD progression via the Wnt pathway. We present the following article in accordance with the ARRIVE reporting checklist (available at https://tlcr.amegroups.com/article/view/10.21037/tlcr-22-593/rc).

Methods

Cell culture and transfection

Human bronchial cells (16HBE) and lung cancer cells (NCI-H1975, H23, H1299, and A549) were purchased from the American Type Culture Collection (ATCC) and were cultured with RPMI 1640 (Gibco, Thermo Fisher Scientific, Waltham, MA, USA) containing 10% fetal bovine serum (FBS, Gibco) at 37 ℃ with 5% CO_2.

The pc-DNA3.1-*PTS* vector was constructed by Tsingke Biotechnology Co., Ltd. (Beijing, China) small interfering RNAs (siRNAs) for *PTS* (si-*PTS*-1 and si-*PTS*-2), siRNA-negative control (si-NC) were synthesized by RiboBio (Guangzhou, China). short hairpin RNAs (shRNAs) for *PTS* (sh-*PTS*) and shRNA-negative control (sh-NC) were synthesized and purified by. Shanghai *Genechem* Co., Ltd. (Shanghai, China) H1299 and A549 cells were transfected with si-NC, si-*PTS*-1, and si-*PTS*-2. H23 cells were transfected with pc-DNA3.1 vector of *PTS*. A549 cells were transfected with cDNA clones of *ATF4*. sh-*PTS* and sh-NC were transfected into A549 cells. The above transfections were carried out using Lipofectamine™ 2000 (Invitrogen, Thermo Fisher Scientific, Waltham, MA, USA) (17).

Clinical samples

LUAD tissue and adjacent tissue were collected from LUAD patients (n=6) admitted to Shandong Provincial Hospital Affiliated to Shandong First Medical University. All patients underwent tumor resection and were not treated with neoadjuvant therapies, including chemotherapy and radiotherapy. The patients were diagnosed with LUAD through pathological examination. The study was conducted in accordance with the Declaration of Helsinki (as revised in 2013). The study was approved by Ethics Committee of Shandong Provincial Hospital Affiliated to Shandong First Medical University (No. 2018-029). Informed written consent was obtained from patients and their families.

Animals and grouping

BALB/c nude mice (n=10, male, 4–5 weeks) were provided by the Jinan Pengyue Experimental Animal Breeding Co., Ltd. (Jinan, China). Mice were divided into two groups: a sh-NC group (n=5) that was injected subcutaneously with cells transfected with sh-NC (5×10^7/mL, 0.1 mL) and a sh-*PTS* group (n=5) that was injected subcutaneously with cells transfected with sh-*PTS* (5×10^7/mL, 0.1 mL). Ten days after inoculation, subcutaneous tumor formation was visually observed, and the length and width of the tumors were observed and recorded at 12, 15, 18, 21, 24, 27, and 30 days. The tumor volume ($V = ab^2/2$) was calculated, and the transplanted tumor growth curve was drawn. The mice were sacrificed, and the transplanted tumor was completely removed, photographed, weighed, and stored at –80 ℃ for further study. The protocol was prepared before the study without registration. Animal experiments were performed under a project license (No. 2018-030) granted by ethics board of Shandong Provincial Hospital Affiliated to Shandong First Medical University, in compliance with Shandong Provincial Hospital Affiliated to Shandong First Medical University guidelines for the care and use of animals.

Western blot

Proteins from clinical samples and cells were extracted with lysate, and protein concentration was tested using a BCA Kit (ab102536, Abcam, USA). Proteins were then taken and subjected to polyacrylamide gel electrophoresis. After electrophoresis, the proteins were electro transferred to a polyvinylidene fluoride membrane (PVDF) and sealed with 5% nonfat milk powder for 1 hour. After that, the membranes were incubated with the following primary antibodies for 24 hours at 4 ℃: PTS (ab96104, Abcam, USA), B-cell lymphoma 2 (Bcl-2; 26593-1-AP, Proteintech, Wuhan), poly-ADP-ribose polymerase (PARP1; ab191217, Abcam, USA), Bcl-2-associated X protein (Bax; #41162, CST, USA), Wnt family member 5A (WNT5A; ab229200, Abcam, USA), glycogen synthase kinase-3 beta (GSK-3β; #12456, CST, USA), β-catenin (ab32572, Abcam, USA), cyclin D1 (ab16663, Abcam, USA) and glyceraldehyde 3-phosphate dehydrogenase (GAPDH; 60004-1-Ig, Proteintech, Wuhan). Next, the membranes were washed with tris-buffered saline with Tween 20 (TBST) and incubated with horseradish peroxidase (HRP)-labeled secondary antibodies for 2 hours and then developed with enhanced chemiluminescence (ECL).

Immunohistochemistry and Ki67 detection

Specimens were fixed with formaldehyde (4%) for 30 min, routinely embedded in paraffin, and sections (5 μm) were prepared. The sections were dewaxed and incubated in 3% H_2O_2 for 5–10 minutes at 37 ℃. After antigen retrieval in a pressure cooker, a *PTS* primary antibody (12150-1-AP, Proteintech) was added, and the sections were incubated overnight at 4 ℃. Then, the sections were incubated with HRP-labeled secondary antibody (37 ℃, 30 minutes). After washing with phosphate-buffered saline (PBS; 2 minutes) for three times, the sections were color developed with diaminobenzidine (DAB) solution (Elabscience, Wuhan, China). PBS was used as a negative control (NC). Ki67 primary antibody (27309-1-AP, Proteintech) was used to detect cell proliferation of subcutaneous tumors.

Quantitative real-time polymerase chain reaction (qRT-PCR)

Total RNA was isolated using Trizol (Invitrogen). cDNA was synthesized using a Reverse Transcription Kit (Vazyme. Nanjing, China). Then, the genes were amplified using a SYBR Green System (Vazyme. Nanjing, China), with *GAPDH* used as the internal reference. Relative gene expression was calculated by the comparative Ct method ($2^{\Delta\Delta CT}$). The sequences of the primers were as follows: *PTS*, F: 5'-TATGAATCTGGCTGATCTCAA-3'; R: 5'-TGCAAAGTATGGCACATCC-3'; *ATF4*, F: 5'-ATGACCGAAATGAGCTTCCTG-3'; R: 5'-GCTGGAGAACCCATGAGGT-3'; *GAPDH*, F: 5'-CCATGGGGAAGGTGAAGGTC-3'; R: 5'-TCGCCCCACTTGATTTTGGA-3'.

Cell Counting Kit-8 (CCK-8)

After transfection, cells (H23, H1299, and A549) were seeded into 96-well plates at 2×10^3 cells/well at 37 ℃ with 5% CO_2. After culturing for 24, 48, 72 and 96 h, 10 μL CCK-8 solutions (Beyotime, Shanghai, China) were added to the plates. After mixing, the cells were incubated 2 hours, and the optical density (OD) of each well was detected at 450 nm.

Flow cytometry

After transfection, H1299 and A549 cells were collected and prepared into a single cell suspension. After washing with precooled PBS, the cells were labeled with fluorescein isothiocyanate (FITC)-Annexin V and propidium iodide

(PI) double antibody (BD Biosciences). Flow cytometry (AccuriC6, BD Biosciences) was used to measure the total apoptosis rate of the cells.

Colony formation assay

After transfection, the cells (H23, H1299, and A549) were digested and inoculated in a 6-well plate. The 6-well plate was taken out after culturing at 37 ℃ with 5% CO_2 for 2 weeks. Methanol (2 mL) was added to each well for 30 minutes. After the methanol was discarded, crystal violet (0.1%, 2 mL) was added to each well for 10 minutes. After the crystal violet was washed off, a picture was taken with a digital camera, and the colonies were counted under a light microscope.

Wound healing assay

After treatment, H23, H1299, and A549 cells were digested and inoculated evenly in 6-well plates overnight. The cell layer was scratched vertically with a sterile pipette tip, and cells scratched by the pipette tip were washed with sterile PBS. The cells were cultured in an incubator (37 ℃, 5% CO_2) for 24 hours, and then the cells were taken out. The width of the scratches was observed and measured under a microscope and photographed. Image J software (National Institutes of Health, Bethesda, MD, USA) was used for data analysis.

Dual-luciferase reporter assay

The sequence of wild type or mutant *PTS* promoter including *ATF4* binding sites was subcloned into a pGL3-luciferase reporter vector. The promoter sequence was synthesized by Genscript Biotech Corporation. The wildtype and mutated PTS promoter were synthesized separately. The luciferase reporter vector and *ATF4* were cotransfected into HEK-293T cells using Lipofectamine 3000 reagent (Invitrogen). After culturing at 37 ℃ for 48 hours, the cells were evaluated by a Dual-Luciferase Reporter Assay System (Promega) following the manufacturer's instructions.

Transwell invasion assay

First, the upper chamber was coated with Matrigel (50 µL), and then the cell suspension (400 µL, $8×10^4$ cells) was added to the upper chamber. Next, RPMI-1640 medium (700 µL,

containing 20% FBS) was added to the lower chamber and cultured at 37 ℃ with 5% CO_2 for 24 hours. After that, the chamber was taken out, and the cells in the upper layer of the pore membrane were wiped off with a cotton swab. The chamber was then fixed with 4% paraformaldehyde for 20 minutes, stained with crystal violet (0.1%, 2 mL, 30 minutes), and counted using a microscope after drying.

Hematoxylin and eosin (HE) staining

Tissue sections were baked at 70 ℃ for 30 minutes and deparaffinized with xylene. The slices were then hydrated with ethanol (95%, 85%, and 75%, 5 minutes per concentration). The sections were stained with hematoxylin, rinsed with water, and differentiated with 1% hydrochloric acid alcohol. Next, the sections were stained with eosin for 10 minutes. After that, the sections were dehydrated with 70%, 80%, 90%, and 100% alcohol for 5 minutes each, rinsed with xylene for 5 minutes, and observed under a microscope.

Terminal deoxynucleotidyl transferase dUTP nick end labeling (TUNEL) assay

Tumor tissues were embedded in paraffin and cut into sections (5 µm). The sections were then analyzed using a TUNEL Apoptosis Assay Kit (Beyotime Biotechnology, Shanghai, China). Pictures were taken under a fluorescence microscope.

Bioinformatics analysis

PTS messenger RNA (mRNA) expression data in the LUAD dataset were downloaded from The Cancer Genome Atlas (TCGA; https://tcga-data.nci.nih.gov/tcga/). *PTS* expression level in LUAD based on individual cancer stages was analyzed by the University of ALabama at Birmingham CANcer data analysis Portal (UALCAN) tool (http://ualcan.path.uab.edu/index.html). The overall survival curve of *PTS* in LUAD was analyzed using Gene Expression Profiling Interactive Analysis (GEPIA; http://gepia.cancer-pku.cn/). The HumanTFDB online prediction tool (http://bioinfo.life.hust.edu.cn/HumanTFDB/#!/tfbs_predict) was used to predict the intersection of transcription factors upstream of *PTS* and the genes positively correlated with *PTS* expression in TCGA-LUAD. Gene Set Enrichment Analysis (GSEA) was performed on the sequenced data using GSEA software (using the dataset h.all.v7.1.symbols.gmt).

Statistical analysis

Data were analyzed using SPSS 21.0 software (IBM Corp., Armonk, NY, USA). Survival analysis was performed using Kaplan-Meier and log-rank tests. *T*-test was used to compare two groups; one-way analysis of variance (ANOVA) was used to compare multiple groups. Correlations were explored using Pearson's correlation analysis. $P<0.01$ and $P<0.05$ were considered statistically significant.

Results

PTS was highly expressed in LUAD

Data analysis of the TCGA dataset using GEPIA found that *PTS* level was significantly up-regulated in LUAD tissue compared to that in normal lung tissue (*Figure 1A*). Meanwhile, *PTS* mRNA expression in LUAD patients was correlated with tumor stage (*Figure 1B*). In addition, higher *PTS* was found to be related with lower overall survival (log-rank $P=0.012$; *Figure 1C*). Furthermore, we found that *PTS* was more highly expressed in LUAD tissues than in normal paracancerous tissue (*Figure 1D,1E*). In addition, *PTS* level in LUAD cells was higher than that in 16HBE cells ($P<0.01$; *Figure 1F,1G*). Taken together, these results suggested that *PTS* was highly expressed in LUAD.

Silencing of PTS inhibited LUAD cell viability and proliferation and accelerated apoptosis

We regulated the expression of intracellular *PTS* by exogenous transfection, and the results indicated that *PTS* level in the si-*PTS*-1 and si-*PTS*-2 groups was markedly lower than that in the si-NC group, while *PTS* level in the *PTS* group was higher than that in the vector group (*Figure 2A*). Furthermore, our results found that down-regulation of *PTS* suppressed cell viability and proliferation and accelerated apoptosis. Moreover, overexpression of *PTS* improved cell viability and proliferation and inhibited apoptosis ($P<0.01$; *Figure 2B-2D*). In addition, the Western blot results found that silencing of *PTS* decreased *Bcl-2*, increased *Bax* level and promoted the cleavage of PARP (*Figure 2E*). Collectively, these results suggested that silencing of *PTS* inhibited LUAD cell proliferation and accelerated apoptosis.

Silencing of PTS inhibited LUAD cell migration and invasion

The results showed that down-regulation of *PTS* suppressed cell migration and invasion. Moreover, overexpression of *PTS* improved cell migration and invasion ($P<0.01$, *Figure 3A-3C*). In addition, the Western blot results revealed that silencing of *PTS* decreased N-cadherin and Vimentin levels but increased E-cadherin level (*Figure 3D*). Collectively, these results suggested that silencing of *PTS* inhibited LUAD cell migration and invasion.

ATF4 is an upstream transcription factor of PTS

Analysis using the HumanTFDB online prediction tool showed that 7 upstream genes were positively correlated with *PTS* level, including *ATF4*, chromobox 3 (*CBX3*), histone deacetylase 2 (*HDAC2*), nuclear transcription factor Y subunit beta (*NFYB*), enhancer of zeste 2 polycomb repressive complex 2 subunit (*EZH2*), ring finger protein 2 (*RNF2*), and zinc finger protein 143 (*ZNF143*; *Figure 4A*). Correlation analysis found that *ATF4* and *PTS* had the highest score and the largest correlation coefficient, so *ATF4* was selected to be included in the study ($R^2=0.18$; *Figure 4B*). Furthermore, we verified the binding of *ATF4* and *PTS* promoter in HEK-293T cells by dual luciferase experiments and found that *ATF4* induced a bigger change in the luciferase activity of the *PTS* promoter-WT than that in the *PTS* promoter-Mut ($P<0.05$; *Figure 4C*). We altered the expression of *ATF4* in A549 cells by transfection and showed that overexpression of *ATF4* increased the expression of *PTS* ($P<0.01$; *Figure 4D-4E*). We further verified the effect of *ATF4* overexpression on LUAD cells and found that up-regulation of *ATF4* reversed the inhibitory effect of *PTS* silencing on cells, leading to the promotion of cell proliferation and invasion and the inhibition of cell apoptosis ($P<0.01$; *Figure 4F-4H*). Taken together, these results suggested that *ATF4* targeted *PTS* promoter and promoted the expression of *PTS* in LUAD.

Knockdown of PTS inhibited the Wnt pathway

We knocked down *PTS* using siRNA in A549 cells and performed transcriptome sequencing (https://www.novogene.com/). The results showed that knockdown of *PTS* affected the expression of lots of genes (*Figure 5A,5B*). Further GSEA analysis found that knockdown of *PTS* inhibited the Wnt pathway (*Figure 5C,5D*). Western blot analysis suggested that down-regulation of *PTS* inhibited the protein levels of *WNT5A*, *GSK-3β*, *β-catenin*, and *cyclin D1*, while up-regulation of *PTS* improved the protein levels of *WNT5A*, *β-catenin*, and *cyclin D1* but decreased
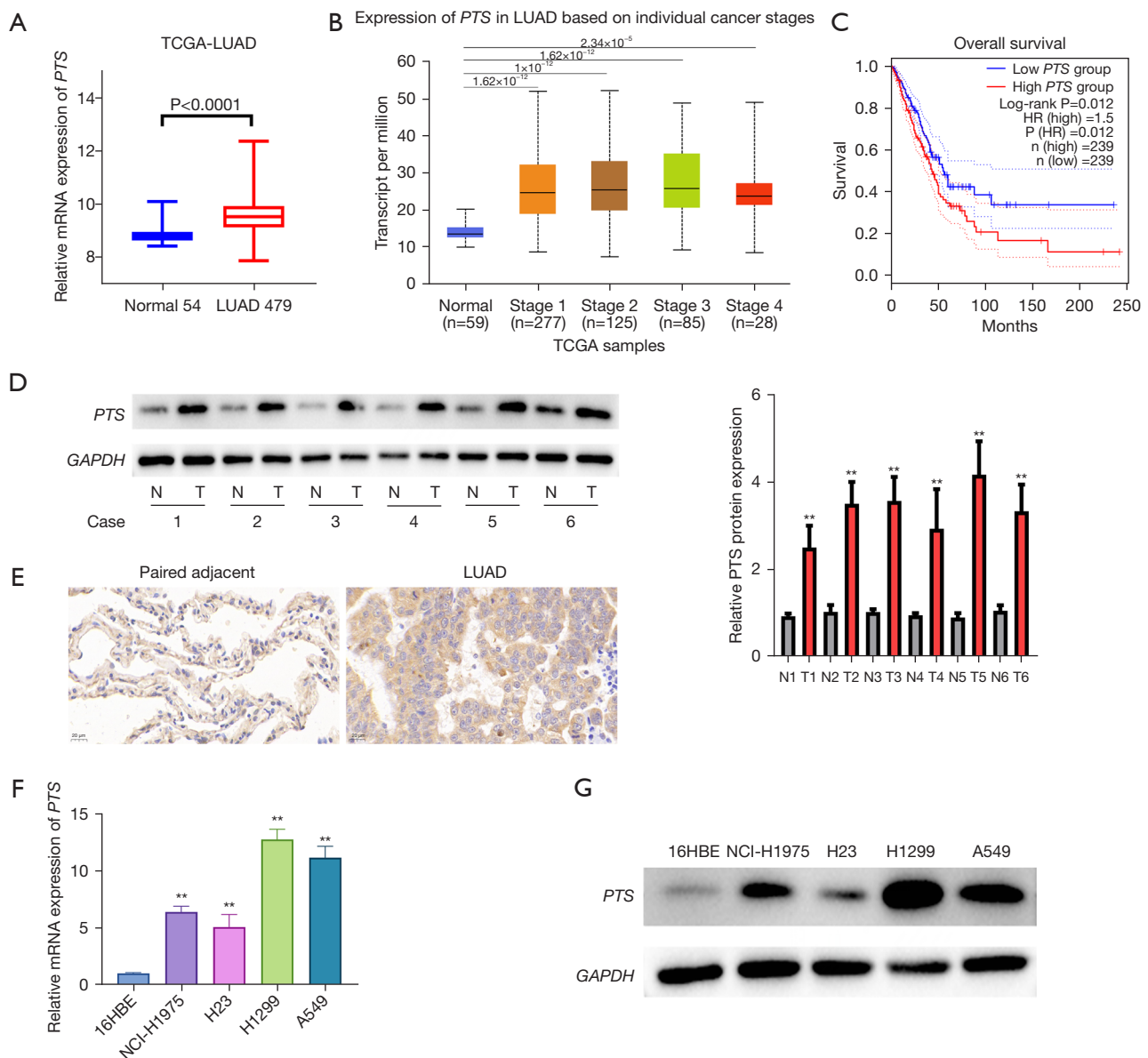
Figure 1 PTS was highly expressed in LUAD. (A) PTS expression level in LUAD in TCGA data. (B) PTS expression level in LUAD based on individual cancer stages. (C) Correlation analysis of PTS level and prognosis of LUAD patients. Expression of PTS level in LUAD tissues was measured by Western blot (D) and immunohistochemistry (stained with PTS antibody; magnification 40×) (E). PTS mRNA and protein level in LUAD cells was tested by qRT-PCR (F) and Western blot (G). **, $P<0.01$, compared with the indicated group. TCGA, The Cancer Genome Atlas; LUAD, lung adenocarcinoma; mRNA, messenger RNA; PTS, 6-pyruvoyl-tetrahydropterin synthase; HR, hazard ratio; GAPDH, glyceraldehyde 3-phosphate dehydrogenase; qRT-PCR, quantitative real-time polymerase chain reaction.

GSK-3β level (Figure 5E). To further verify the effect of PTS on the Wnt pathway, cells were treated with Wnt pathway activator BML-284 (1 µmol/L, MedChemExpress, Monmouth Junction, NJ, USA). The results showed that

down-regulation of PTS inhibited the protein levels of WNT5A, β-catenin, and cyclin D1 but increased GSK-3β level (Figure 5F). Furthermore, BML-284 reversed the functional effects on LUAD cells of silencing PTS, leading to
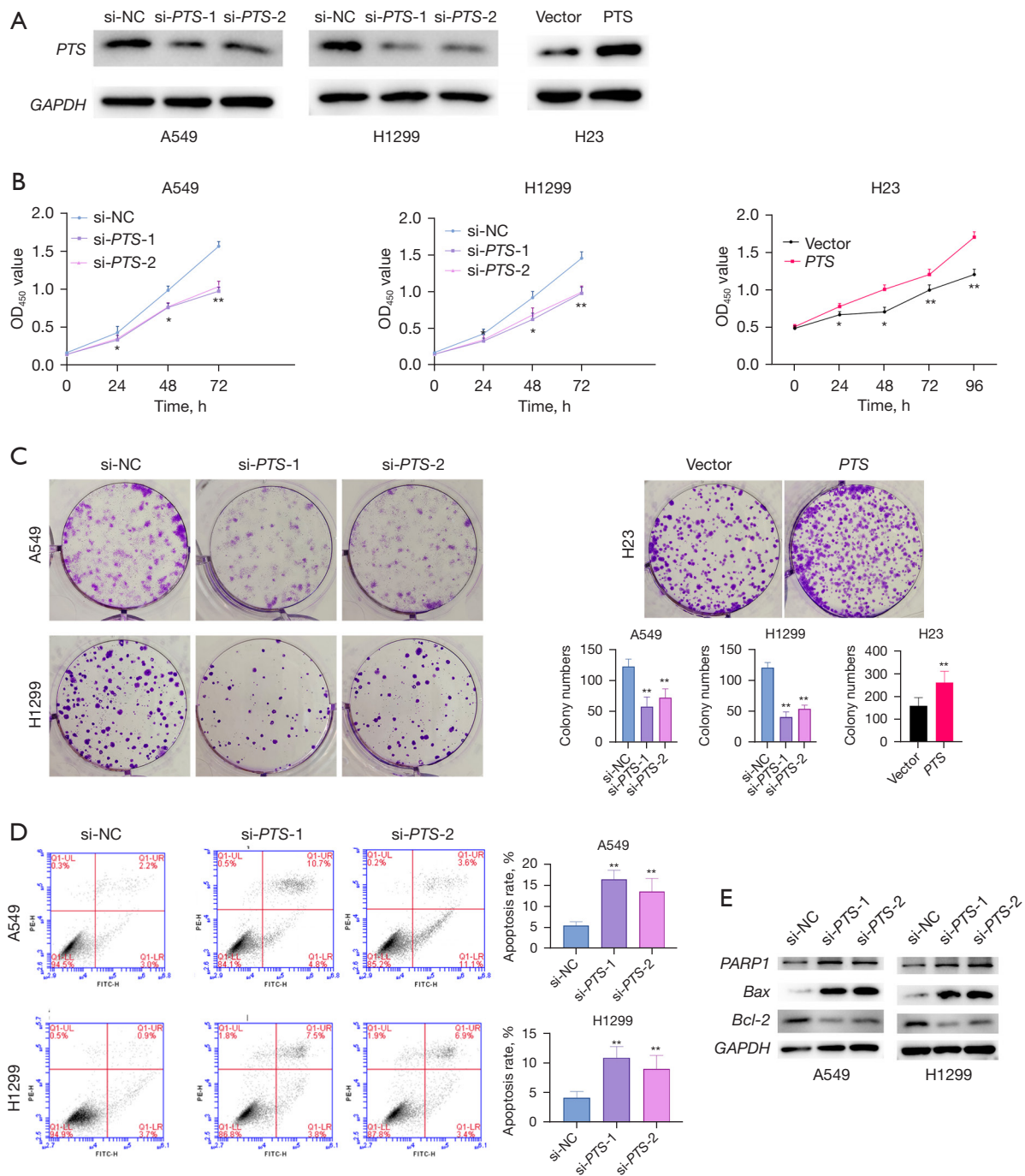
Figure 2 Silencing of *PTS* inhibited LUAD cell viability and proliferation and accelerated apoptosis. (A) *PTS* protein level was tested by Western blot. Cell viability and apoptosis were determined by CCK-8 (B), colony formation assay (stained with crystal violet; magnification 100×) (C), and flow cytometry (D), respectively. (E) Levels of *Bcl-2*, *PARP1*, and *Bax* were tested by Western blot. *, P<0.05; **, P<0.01, compared with the si-NC group or vector group. *PTS*, 6-pyruvoyl-tetrahydropterin synthase; *GAPDH*, glyceraldehyde 3-phosphate dehydrogenase; si-NC, siRNA-negative control; siRNA, small interfering RNA; si-PTS, siRNA for *PTS*; OD, optical density; *PARP1*, poly-ADP-ribose polymerase; *Bax*, *Bcl-2*-associated X protein; *Bcl-2*, B-cell lymphoma 2; LUAD, lung adenocarcinoma; CCK-8, Cell Counting Kit-8.
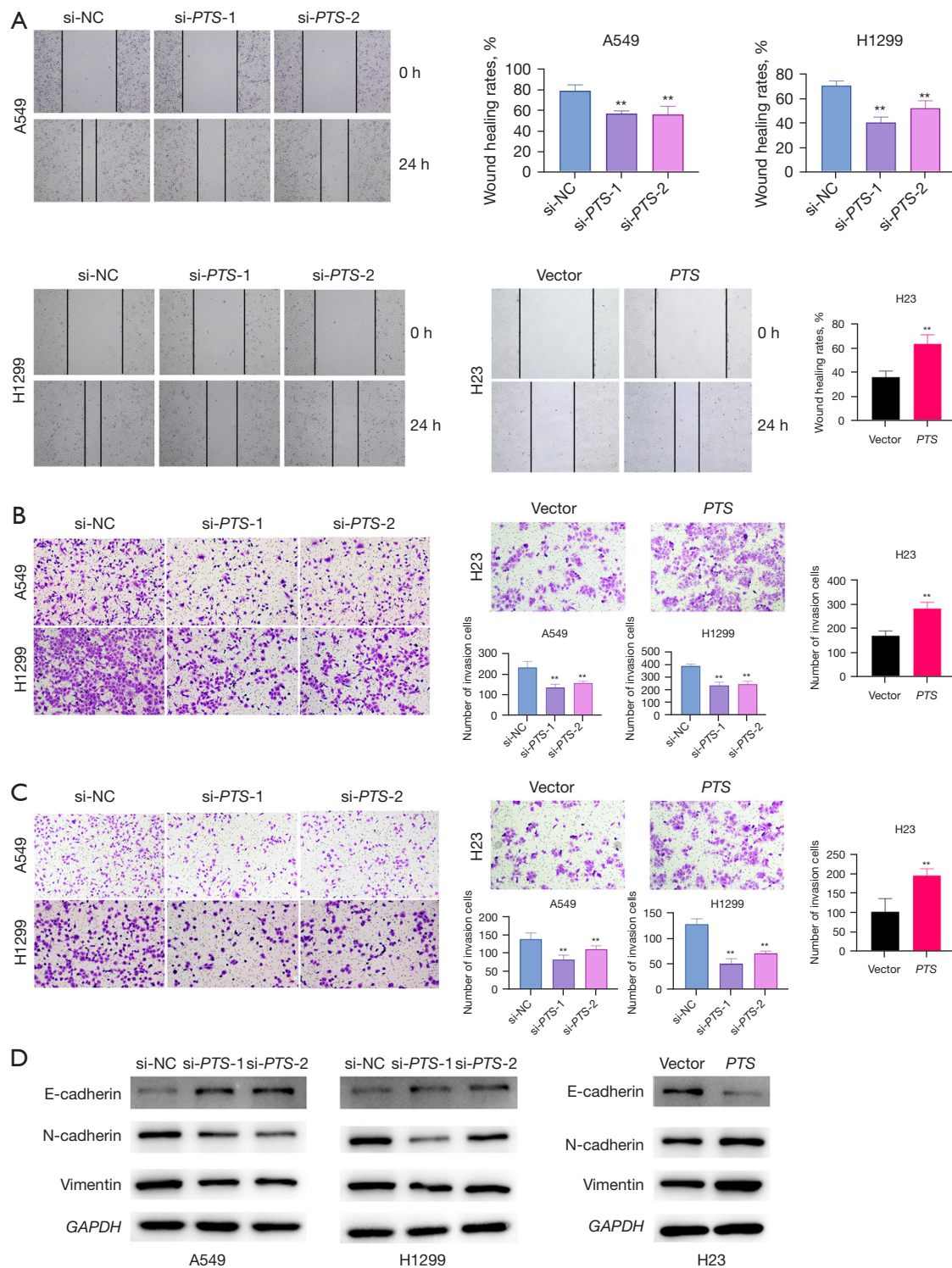
Figure 3 Silencing of *PTS* inhibited LUAD cell migration and invasion. (A) Cell migration was tested by wound healing assay (magnification 4×). Transwell assay was used to test cell migration (B) (stained with crystal violet; magnification 10×) and invasion (C) (stained with crystal violet; magnification 10×). (D) Levels of E-cadherin, vimentin and N-cadherin were tested by Western blot. **, P<0.01, compared with the indicated group. si-NC, siRNA-negative control; siRNA, small interfering RNA; si-*PTS*, siRNA for *PTS*; *PTS*, 6-pyruvoyl-tetrahydropterin synthase; *GAPDH*, glyceraldehyde 3-phosphate dehydrogenase; LUAD, lung adenocarcinoma.
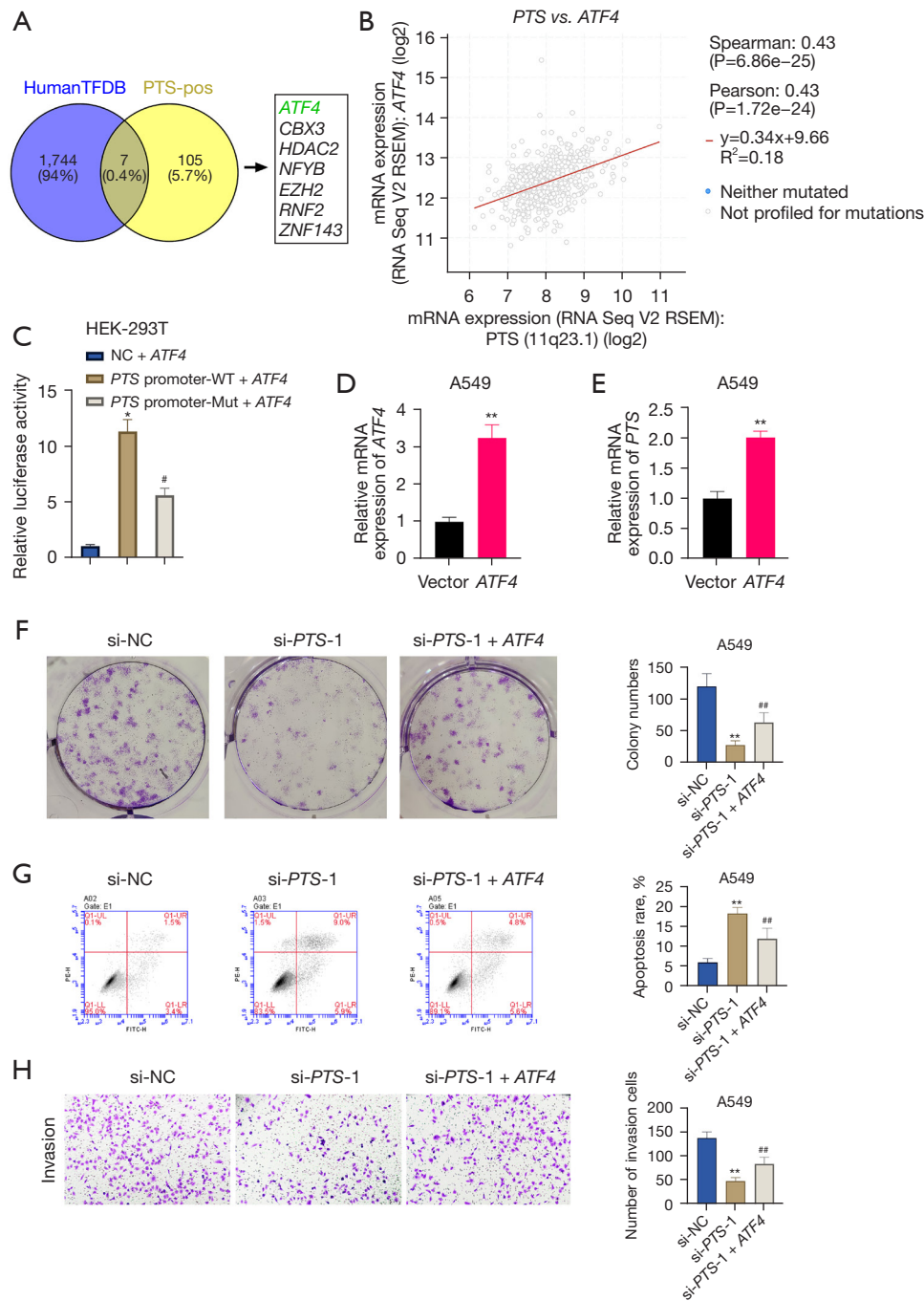
Figure 4 *ATF4* is an upstream transcription factor of *PTS*. (A) *PTS* upstream transcription factors were predicted by HumanTFDB. (B) Linear analysis of *PTS* and *ATF4*. (C) Interaction between *ATF4* and *PTS* was verified by dual luciferase assay. *ATF4* mRNA (D) and *PTS* mRNA (E) were tested by qRT-PCR. Cell proliferation, apoptosis, and invasion were tested by colony formation assay (stained with crystal violet; magnification 100×) (F), flow cytometry (G), and transwell assay (stained with crystal violet; magnification 200×) (H). #, P<0.05, ##, P<0.05, compared with the si-*PTS*-1 group. *, P<0.05; **, P<0.01, compared with the si-NC group. *PTS*, 6-pyruvoyl-tetrahydropterin synthase; *ATF4*, activating transcription factor 4; *CBX3*, chromobox 3; *HDAC2*, histone deacetylase 2; *NFYB*, nuclear transcription factor Y subunit beta; *EZH2*, enhancer of zeste 2 polycomb repressive complex 2 subunit; *RNF2*, ring finger protein 2; *ZNF143*, zinc finger protein 143; NC, negative control; WT, wild type; Mut, mutant; mRNA, messenger RNA; si-NC, siRNA-negative control; siRNA, small interfering RNA; si-*PTS*, siRNA for *PTS*; qRT-PCR, quantitative real-time polymerase chain reaction.
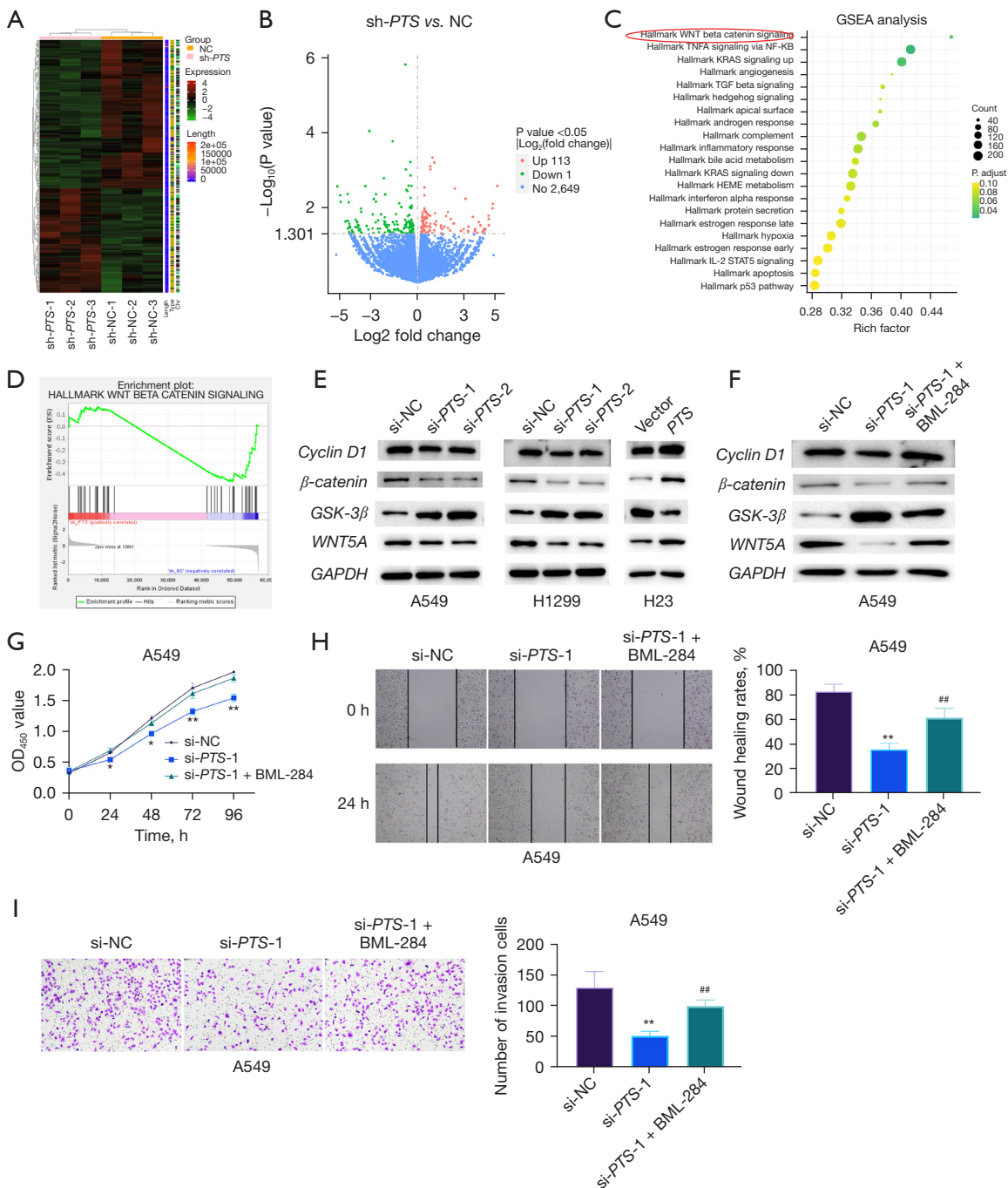
Figure 5 Knockdown of *PTS* inhibited the Wnt pathway. (A,B) Transcriptome sequencing analysis after knockdown of *PTS*. (C,D) GSEA of *PTS*. (E,F) Protein levels of *WNT5A*, *GSK-3β*, *β-catenin*, and *cyclin D1* were tested by Western blot. Cell viability, migration, and proliferation were detected using CCK-8 (G), wound healing assay (measured under a microscope, magnification 200×) (H), and transwell assay (stained with crystal violet; magnification 200×) (I). ##, P<0.05, compared with the si-*PTS*-1 group. *, P<0.05; **, P<0.01, compared with the si-NC group. sh-NC, shRNA-negative control; shRNA, short hairpin RNA; sh-*PTS*, shRNA for *PTS*; *PTS*, 6-pyruvoyl-tetrahydropterin synthase; GSEA, Gene Set Enrichment Analysis; *GSK-3β*, glycogen synthase kinase-3 beta; *WNT5A*, Wnt family member 5A; *GAPDH*, glyceraldehyde 3-phosphate dehydrogenase; si-NC, siRNA-negative control; siRNA, small interfering RNA; si-*PTS*, siRNA for *PTS*; CCK-8, Cell Counting Kit-8.
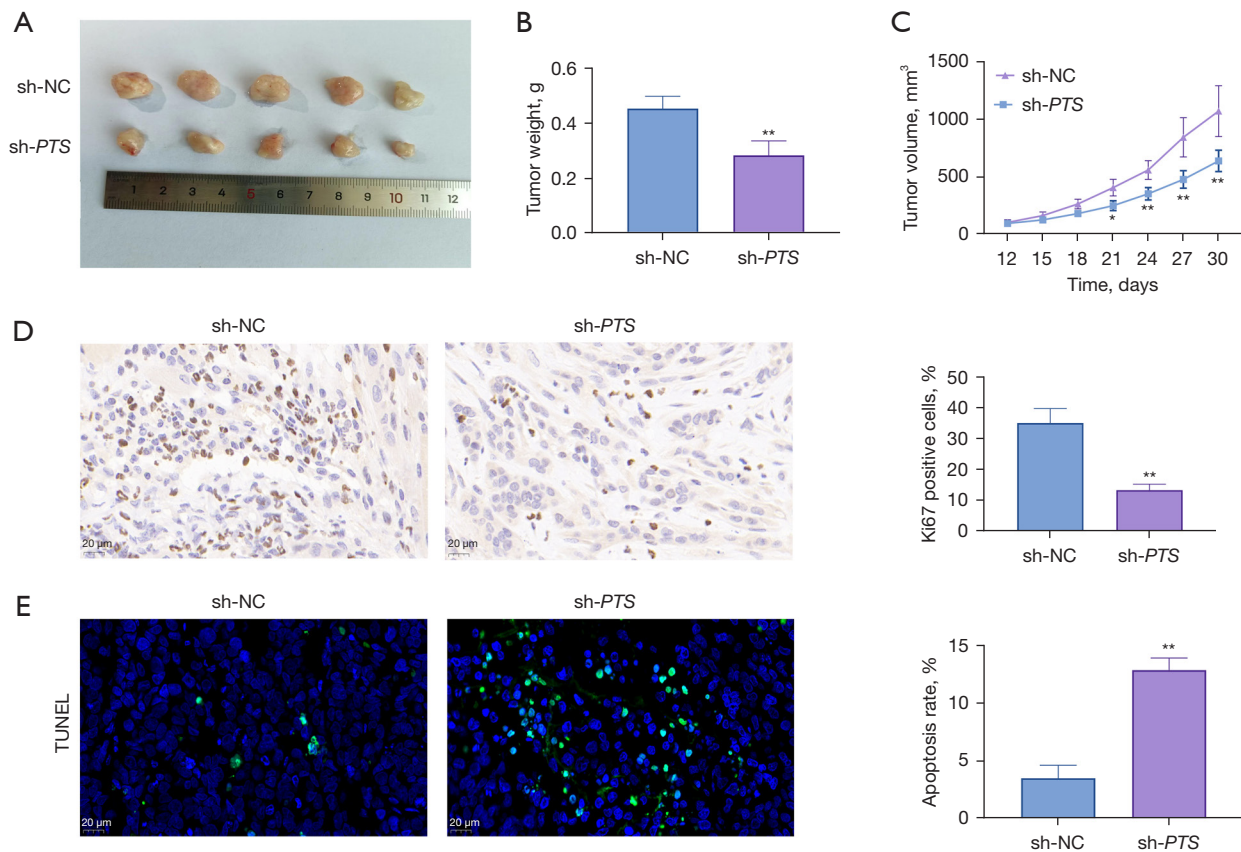
Figure 6 Silencing of *PTS* inhibited tumor formation in mice. Subcutaneous xenograft (A), weight (B), and volume (C) of tumor were monitored. (D) Ki67 assay for proliferation (magnification 200×). (E) Apoptosis was measured by TUNEL (magnification 200×). *, P<0.05; **, P<0.01, compared with the sh-NC group. sh-NC, shRNA-negative control; shRNA, short hairpin RNA; sh-*PTS*, shRNA for *PTS*; *PTS*, 6-pyruvoyl-tetrahydropterin synthase; TUNEL, terminal deoxynucleotidyl transferase dUTP nick end labeling.

enhanced cell viability and the promotion of cell migration and invasion (P<0.01; *Figure 5G-5I*). In summary, down-regulation of *PTS* inhibited cell viability, migration, and proliferation by inhibiting the Wnt pathway.

Silencing of PTS inhibited tumor formation in mice

As demonstrated in *Figure 6A-6C*, silencing of *PTS* markedly suppressed the weight and volume of tumors in the sh-*PTS* group in contrast with those in sh-NC group (P<0.01). The results of Ki67 assay found that the Ki67-positive rate in the sh-*PTS* group was markedly decreased than that in the sh-NC group (P<0.01; *Figure 6D*). However, the apoptosis rate of the sh-*PTS* group was markedly increased than that of the sh-NC group (P<0.01; *Figure 6E*). In summary, silencing of *PTS* inhibited tumor development in mice.

Discussion

According to the 2018 global tumor statistics, approximately 18.19 million novel malignant tumors cases and 9.6 million deaths occurred worldwide, with lung cancer accounting for 11.6% of the incidence rate and 18.4% of the fatality rate (18). LUAD cells are mainly characterized by immortality, migration, and loss of contact inhibition, which are the main reasons for tumor refractory treatment (19). Studies have found that chromosomal changes, gene mutations, epigenetic changes, and other gene-level changes play a vital role in the occurrence and development of LUAD. At the same time, these gene changes also provide potential targets for the treatment of the disease (20-22). In this study, TCGA data analysis indicated that *PTS* is highly expressed in LUAD, and that high *PTS* is related to advanced stage and lower overall survival. Meanwhile,

PTS was found to be up-regulated in LUAD tissue and cells. Hence, we speculated that *PTS* might be a novel potential target of LUAD, and we carried out experiments to study its effect and mechanism on LUAD. *PTS* has been extensively studied as an important cofactor for enzymes such as hepatic phenylalanine hydroxylase (23,24). Similarly, knockdown of *PTS* has been reported to suppress colorectal tumor cells growth (9).

Our study found that in LUAD, *ATF4* level was positively correlated with *PTS*, and up-regulation of *ATF4* reversed the inhibitory effect of silencing of *PTS* on LUAD cells. *ATF4* has been reported to be up-regulated in lung cancer cells and to promote cancer progression (12), which is consistent with our study. Taken together, our results suggest that *PTS* is activated by *ATF4* and promotes LUAD progression.

Further GSEA analysis showed that the Wnt pathway was inhibited by down-regulation of *PTS* in LUAD. To verify this finding, we found that down-regulation of *PTS* inhibited the levels of Wnt pathway downstream target proteins (*WNT5A*, *β-catenin*, and *cyclin D1*). The Wnt pathway is often abnormally activated and regulates tumor proliferation, migration, and invasion in the occurrence and development of LUAD (25). Interestingly, we found that silencing *PTS* inhibited LUAD development via inhibiting the Wnt pathway. Similarly, chromobox 4 has been found to promote tumorigenesis of LUAD through activation of the Wnt/*β-catenin* pathway (26). Tumor endothelial marker 8 has also been found to facilitate LUAD proliferation and metastasis via the Wnt/*β-catenin* pathway (27). We also explored the impact of *PTS* on LUAD *in vivo*. Down-regulation of *PTS* inhibited tumor growth in the mouse model, which was in agreement with our findings in cells. One limitation of this study is that although it appears that *PTS* is activated by *ATF4* and this promotes LUAD's progression by regulating the Wnt pathway, further investigation on the mechanism *in vivo* is missing, something in our follow-up research agenda.

Conclusions

Our study is the first work to investigate the expression and impacts of *PTS* in LUAD. Higher *PTS* is associated with poor prognosis. *PTS* is activated by *ATF4* and facilitates LUAD progression by regulating the Wnt pathway, indicating that *PTS* may be a novel target for the treatment of LUAD.

Footnote

Reporting Checklist: The authors have completed the ARRIVE reporting checklist. Available at https://tlcr.amegroups.com/article/view/10.21037/tlcr-22-593/rc

Data Sharing Statement: Available at https://tlcr.amegroups.com/article/view/10.21037/tlcr-22-593/dss

Conflicts of Interest: All authors have completed the ICMJE uniform disclosure form (available at https://tlcr.amegroups.com/article/view/10.21037/tlcr-22-593/coif). WM reports funding support from the Natural Science Foundation of Shandong Province (No. ZR2020MH233 to WM). WD reports funding support from the National Natural Science Foundation of China (No. 81802282 to WD). The other authors have no conflicts of interest to declare.

Ethical Statement: The authors are accountable for all aspects of the work in ensuring that questions related to the accuracy or integrity of any part of the work are appropriately investigated and resolved. The study was conducted in accordance with the Declaration of Helsinki (as revised in 2013). The study was approved by Ethics Committee of Shandong Provincial Hospital Affiliated to Shandong First Medical University (No. 2018-029). Informed written consent was obtained from patients and their families. Animal experiments were performed under a project license (No. 2018-030) granted by ethics board of Shandong Provincial Hospital Affiliated to Shandong First Medical University, in compliance with Shandong Provincial Hospital Affiliated to Shandong First Medical University guidelines for the care and use of animals.

Open Access Statement: This is an Open Access article distributed in accordance with the Creative Commons Attribution-NonCommercial-NoDerivs 4.0 International License (CC BY-NC-ND 4.0), which permits the non-

commercial replication and distribution of the article with the strict proviso that no changes or edits are made and the original work is properly cited (including links to both the formal publication through the relevant DOI and the license). See: https://creativecommons.org/licenses/by-nc-nd/4.0/.

References

1. Siegel RL, Miller KD, Fuchs HE, et al. Cancer Statistics, 2021. CA Cancer J Clin 2021;71:7-33.
2. Brustugun OT, Grønberg BH, Fjellbirkeland L, et al. Substantial nation-wide improvement in lung cancer relative survival in Norway from 2000 to 2016. Lung Cancer 2018;122:138-45.
3. Warth A, Muley T, Meister M, et al. The novel histologic International Association for the Study of Lung Cancer/American Thoracic Society/European Respiratory Society classification system of lung adenocarcinoma is a stage-independent predictor of survival. J Clin Oncol 2012;30:1438-46.
4. Miles B, Mackey JD. Epidermal Growth Factor Receptor Tyrosine Kinase Inhibitors and Lung Cancer: History, Epidemiology, and Market Outlook. Cureus 2021;13:e13470.
5. Pacini L, Jenks AD, Lima NC, et al. Targeting the Fibroblast Growth Factor Receptor (FGFR) Family in Lung Cancer. Cells 2021;10:1154.
6. Zhao Z, Zhang N, Li A, et al. Insulin-like growth factor-1 receptor induces immunosuppression in lung cancer by upregulating B7-H4 expression through the MEK/ERK signaling pathway. Cancer Lett 2020;485:14-26.
7. Thöny B, Leimbacher W, Bürgisser D, et al. Human 6-pyruvoyltetrahydropterin synthase: cDNA cloning and heterologous expression of the recombinant enzyme. Biochem Biophys Res Commun 1992;189:1437-43.
8. Manzoni F, Salvatici E, Burlina A, et al. Retrospective analysis of 19 patients with 6-Pyruvoyl Tetrahydropterin Synthase Deficiency: Prolactin levels inversely correlate with growth. Mol Genet Metab 2020;131:380-9.
9. Zhao Q, Zheng K, Ma C, et al. PTPS Facilitates Compartmentalized LTBP1 S-Nitrosylation and Promotes Tumor Growth under Hypoxia. Mol Cell 2020;77:95-107.e5.
10. Lorenz NI, Sittig ACM, Urban H, et al. Activating transcription factor 4 mediates adaptation of human glioblastoma cells to hypoxia and temozolomide. Sci Rep 2021;11:14161.
11. Ameri K, Harris AL. Activating transcription factor 4. Int

J Biochem Cell Biol 2008;40:14-21.
12. Du J, Liu H, Mao X, et al. ATF4 promotes lung cancer cell proliferation and invasion partially through regulating Wnt/β-catenin signaling. Int J Med Sci 2021;18:1442-8.
13. Zhang J, Li C, Zhang L, et al. Andrographolide Induces Noxa-Dependent Apoptosis by Transactivating ATF4 in Human Lung Adenocarcinoma Cells. Front Pharmacol 2021;12:680589.
14. Sharma RP. Wingless a new mutant in Drosophila melanogaster. Drosophila Information Service 1973. Available online: http://repository.ias.ac.in/71006/1/71006.pdf
15. He S, Tang S. WNT/β-catenin signaling in the development of liver cancers. Biomed Pharmacother 2020;132:110851.
16. Clevers H. Wnt/beta-catenin signaling in development and disease. Cell 2006;127:469-80.
17. Wang Y, Wo Y, Lu T, et al. Circ-AASDH functions as the progression of early stage lung adenocarcinoma by targeting miR-140-3p to activate E2F7 expression. Transl Lung Cancer Res 2021;10:57-70.
18. Bray F, Ferlay J, Soerjomataram I, et al. Global cancer statistics 2018: GLOBOCAN estimates of incidence and mortality worldwide for 36 cancers in 185 countries. CA Cancer J Clin 2018;68:394-424.
19. Fu F, Zhang Y, Gao Z, et al. Development and validation of a five-gene model to predict postoperative brain metastasis in operable lung adenocarcinoma. Int J Cancer 2020;147:584-92.
20. Wu X, Sui Z, Zhang H, et al. Integrated Analysis of lncRNA-Mediated ceRNA Network in Lung Adenocarcinoma. Front Oncol 2020;10:554759.
21. Ma L, Chen T, Zhang X, et al. The m6A reader YTHDC2 inhibits lung adenocarcinoma tumorigenesis by suppressing SLC7A11-dependent antioxidant function. Redox Biol 2021;38:101801.
22. Soria JC, Ohe Y, Vansteenkiste J, et al. Osimertinib in Untreated EGFR-Mutated Advanced Non-Small-Cell Lung Cancer. N Engl J Med 2018;378:113-25.
23. Gundorova P, Kuznetcova IA, Baydakova GV, et al. BH4-deficient hyperphenylalaninemia in Russia. PLoS One 2021;16:e0249608.
24. Chaiyasap P, Ittiwut C, Srichomthong C, et al. Massive parallel sequencing as a new diagnostic approach for phenylketonuria and tetrahydrobiopterin-deficiency in Thailand. BMC Med Genet 2017;18:102.
25. Lei L, Wang Y, Li ZH, et al. PHLDA3 promotes lung

adenocarcinoma cell proliferation and invasion via activation of the Wnt signaling pathway. Lab Invest 2021;101:1130-41.

26. Wang Z, Fang Z, Chen G, et al. Chromobox 4 facilitates tumorigenesis of lung adenocarcinoma through the Wnt/β-catenin pathway. Neoplasia 2021;23:222-33.

27. Ding C, Liu J, Zhang J, et al. Tumor Endothelial Marker 8 Promotes Proliferation and Metastasis via the Wnt/β-Catenin Signaling Pathway in Lung Adenocarcinoma. Front Oncol 2021;11:712371.

Transl Lung Cancer Res 2022;11(9):1912-1925 | https://dx.doi.org/10.21037/tlcr-22-593